Superoxide Radical Anion Adduct of 5,5-Dimethyl-1-pyrroline *N*-Oxide (DMPO). 3. Effect of Mildly Acidic pH on the Thermodynamics and Kinetics of Adduct Formation

Randy A. Burgett, Xiaofeng Bao, and Frederick A. Villamena*

Department of Pharmacology and Davis Heart and Lung Research Institute, The Ohio State University, Columbus, Ohio 43210

Received: November 8, 2007; In Final Form: December 19, 2007

The nitrone, 5,5-dimethylpyrroline *N*-oxide (DMPO), is a commonly used spin trap for the detection of superoxide radical anion ($O_2^{\bullet-}$) using electron paramagnetic resonance spectroscopy. This work investigates the reactivity of DMPO to $O_2^{\bullet-}$ in mildly acidic pH (5.0−7.0). Mild acidity is characteristic of acidosis and has been observed in hypoxic systems, e.g., ischemic organs and cancer cells. Although the established pK_a for $O_2^{\bullet-}$ is 4.8, the pK_a for DMPO is unknown. The pK_a of the conjugate acid of DMPO was determined to be 6.0 using potentiometric, spectrophotometric, ^{1}H and ^{13}C NMR, and computational methods. ^{1}H and ^{13}C NMR were employed to investigate the site of protonation. An alternative mechanism for the spin trapping of $O_2^{\bullet-}$ in mildly acidic pH was proposed, which involves protonation of the oxygen to form the *N*-hydroxy imino cation and subsequent addition of $O_2^{\bullet-}$. The exoergicity of $O_2^{\bullet-}$ addition to protonated DMPO was rationalized using density functional theory (DFT) at the PCM/B3LYP/6-31+G**//B3LYP/6-31G* level of theory.

I. Introduction

Reactive oxygen species (ROS) in low concentrations play a vital role in the regulation of physiological processes and are central in the initiation of pathological events in unregulated concentrations.[1,2] Studies show[3−5] that the ischemic period (a condition by which the tissues or organs are deprived of blood flow) and during immediate reperfusion exhibit an enhanced oxygen radical production and are accompanied by acidosis[6] in which the extracellular or intracellular pH usually ranges from 6.00 to 7.35.[7] Moreover, tumor cell microenvironment is characterized by hypoxia and acidosis, which have negative implications for their effective treatment.[8−10]

Nitrones, such as 5,5-dimethylpyrroline *N*-oxide (DMPO) and α-phenyl-*tert*-butylnitrone (PBN), have exhibited pharmacological activity such as in the treatment of neurodegenerative disease,

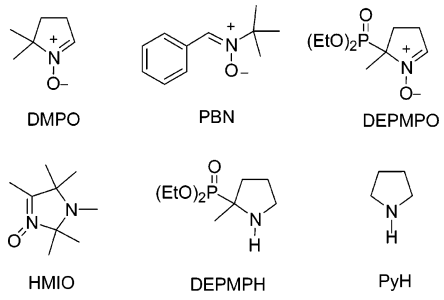

acute stroke, and cardioprotection from ischemia−reperfusion injury.[11−20] Free radicals such as those derived from the superoxide radical anion ($O_2^{\bullet-}$) has been shown to be generated from isolated perfused heart during post-ischemia.[5] Although the spin trapping of free radicals by DMPO may explain their cardioprotective property against reperfusion injury, studies in this regard are conflicting. For example, using Langendorff rat heart reperfusion preparations, Bradamente et al.[21] showed that DMPO in millimolar concentrations did not show cardioprotection from ischemia−reperfusion injury, and Pietri et al.[22,23] and Tosaki et al.[24−26] have shown otherwise. The mechanism of the cardioprotective property of DMPO was believed to be due to its direct radical scavenging property because studies on structurally related compounds such as HMIO[26] or PyH,[23] which are non spin trapping, did not exhibit improvement in cardiac function. However, the presence of phosphonate group in a spin trap such as DEPMPO, as well as non spin traps, DEPMPH and MeP(O)(OEt)$_2$, has been demonstrated to play a critical role in cardioprotection.[23] Therefore, there are issues in terms of which functional group (or structural feature) is responsible for cardioprotection. Other mechanisms of the cardioprotection of DMPO have been linked to its direct effect on Ca^{2+} channels;[27,28] or increase in nitric oxide bioavailability,[29,30] hence, the mechanism of the pharmacological activity of DMPO is more complex than simple radical scavenging.

The mechanism of nitrone antioxidant activity is intriguing because at neutral pH, the reactivity of $O_2^{\bullet-}$ to DMPO is slow, with a second-order rate constant of only 2.0 M^{-1} s^{-1}; however, at acidic pH, the reactivity is ∼27 or ∼10^3 M^{-1} s^{-1} at pH 6.2[31] and 5.0,[32] respectively. The high reactivity of $O_2^{\bullet-}$ to DMPO in acidic pH was proposed to be due to the protonation of $O_2^{\bullet-}$ to form hydroperoxyl radical ($HO_2^{\bullet}$), because the pK_a for $O_2^{\bullet-}$ and $HO_2^{\bullet}$ is 4.8[33] and 4.4[34] and the fact that $HO_2^{\bullet}$ is a stronger oxidizer than $O_2^{\bullet-}$ ($E^{o\prime}$ = 1.06 and 0.94 V, respectively).[35] The higher reactivity of $HO_2^{\bullet}$ to DMPO compared to $O_2^{\bullet-}$ was theoretically rationalized and the predicted rate constants in aqueous phase for the $O_2^{\bullet-}$ [36] or $HO_2^{\bullet}$ [37] addition to DMPO was found to be 5.9 × 10^{-5} and 285 M^{-1} s^{-1}, respectively, at the PCM/B3LYP/6-31+G**//B3LYP/6-31G* level of theory. At the same level of theory, the calculated thermodynamic data in aqueous phase also show a more facile addition of $HO_2^{\bullet}$ [37] to

* Corresponding author. E-mail: Frederick.Villamena@osumc.edu. Fax: 614-688-0999.

10.1021/jp7107158 CCC: $40.75
Published on Web 02/28/2008

DMPO compared to $O_2^{\bullet-}$ [36] with ΔG_{rxn} of −4.6 and 11.9 kcal/mol, respectively.

Because acidosis plays a critical role in the initiation of brain[38] or heart[39−41] damage during ischemia and because production of $O_2^{\bullet-}$ is ubiquitous during these pathophysiological events, spin trapping of $O_2^{\bullet-}$ by nitrones in mildly acidic medium is, therefore, relevant. The reported spin trapping rate for $O_2^{\bullet-}$ at pH 6 is an order of a magnitude higher than at pH 7, but complete protonation of $O_2^{\bullet-}$ at pH 6 may not occur due to its pK_a of 4.8. It is, therefore, important to investigate the basicity of a model nitrone, DMPO, to shed insight into the rate of $O_2^{\bullet-}$ addition to DMPO at pH above the pK_a of $O_2^{\bullet-}$.

II. Experimental Methods

A. Ionization Constant Determination. ***(a) Potentiometric Titration.*** DMPO (99.9%) was purchased from Dojindo without further purification. A 10 mL DMPO stock solution (0.04 mM) was prepared using double distilled deionized water containing 1 μM NaCl to stabilize the pH reading. The pH of the starting solution of 2 mL DMPO (0.04 mM) was slightly basic (7.4) and was titrated with 1.01 mM HCl (standardized using Na_2CO_3) at 5 μL increments. The resulting pH's were monitored using a pH microelectrode calibrated at pH 4.00, 7.00, and 10.00. No activity calculations were necessary because the titration was preformed at very low ionic strength. Experiments were preformed in triplicate measurements.

(b) Spectrophotometric Titration. A 20 mL solution of DMPO (100 μM) in double distilled deionized water was prepared and titrated with 2 μL increment of 1.01 mM HCl. Two milliliters of the solution was taken at every pH change of ∼0.25 then UV absorbance was measured. Experiments were preformed in duplicate measurements.

B. NMR Measurements. Two mL solution of DMPO (15 mM) was prepared in D_2O at pH's 5.10, 6.00, 6.85, and 7.00 using D_2SO_4 (no acid was used for pH 7.0) and ^{1}H NMR spectra were acquired. However, for ^{13}C NMR, solutions at pH's 4.90, 6.00, 6.50, and 7.10 (without acid) were prepared using higher DMPO concentration of 50 mM.

C. General Computational Methods. ***(a) General Details.*** Density functional theory[42,43] was applied in this study to determine the optimized geometry, vibrational frequencies, and single-point energy of all stationary points.[44−47] The effect of aqueous solvation was also investigated using the polarizable continuum model (PCM).[48−52] All calculations were performed using Gaussian 03[53] at the Ohio Supercomputer Center. Single-point energies were obtained at the B3LYP/6-31+G** level based on the optimized B3LYP/6-31G* geometries, and the B3LYP/6-31+G**//B3LYP/6-31G* wave functions were used for Natural Population Analyses (NPA).[54] These calculations used six Cartesian d functions. Geometry optimization with diffuse functions at the B3LYP/6-311+G* level of theory was performed to account for the negative charge character of the species being investigated using five d (pure) functions for these calculations. Stationary points for nitrones and its respective adducts as well as protonated forms have zero imaginary vibrational frequency as derived from a vibrational frequency analysis (B3LYP/6-31G*). A scaling factor of 0.9806 was used for the zero-point vibrational energy (ZPE) corrections for the B3LYP/6-31G* and the B3LYP/6-311+G* levels.[55] Spin contamination for all of the stationary point of the radical structures was negligible, i.e., $\langle S^2 \rangle = 0.75$.

(b) Calculation of pK_a. Ionization constants for various protonated nitrones were predicted according to the method previously described.[56] Geometry optimization of the protonated and unprotonated nitrones was carried out at the B3LYP/6-311+G* level of theory. Calculated free energies of solvation were based on the bottom-of-the-well energies at the PCM/B3LYP/6-311+G* using the scrf=oldpcm command.

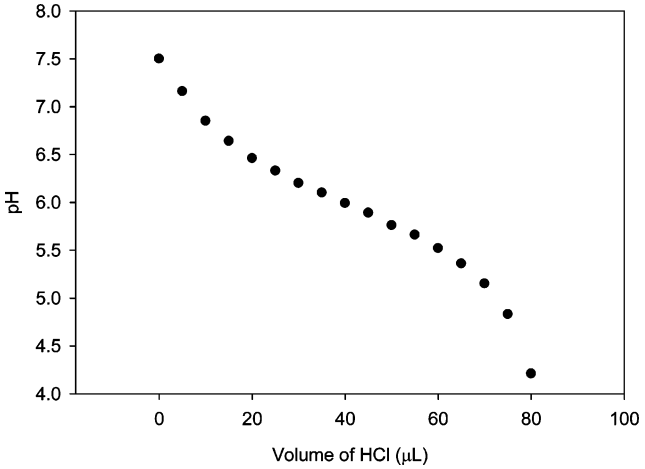

Figure 1. Potentiometric titration of 0.04 mM DMPO with 1 mM HCl in water at 25 °C.

SCHEME 1: pK_a's for Various *N*-Oxides

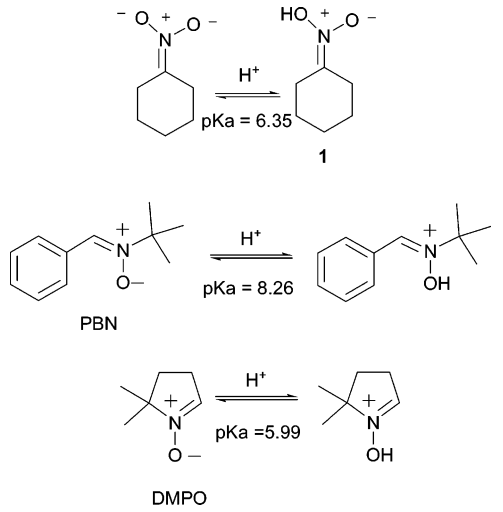

III. Results and Discussion

A. Determination of pK_a for DMPO.

(a) Potentiometric Titration. Figure 1 shows the potentiometric titration curve of 0.04 mM DMPO with 1 mM HCl. The ionization constant of the conjugate acid of DMPO was calculated according to the method described by Albert and Serjeant[57] (see Tables S1−S3 of Supporting Information) using eq 1 and gave a pK_a of 5.99 ± 0.02 (n = 30) at 25 °C, where

$$pK_a = pH + \log \frac{[DMPO-H^+]}{[DMPO]} \qquad (1)$$

[DMPO−H$^+$] and [DMPO] correspond to the concentrations of the protonated and unprotonated DMPO, respectively. The pK_a of ∼6.0 indicates the mildly acidic property of DMPO and resembles that of some carboxylic acids[58] and *aci*-form of the nitronic acid, **1**[59] (Scheme 1). The observed pK_a for DMPO is lower compared to that observed for PBN of 8.26[59] due to mesomeric effects of the conjugated phenyl moiety (Scheme 2), therefore, stabilizing the conjugate acid form. Also, the electron donating inductive effect of the *tert*-butyl group of PBN

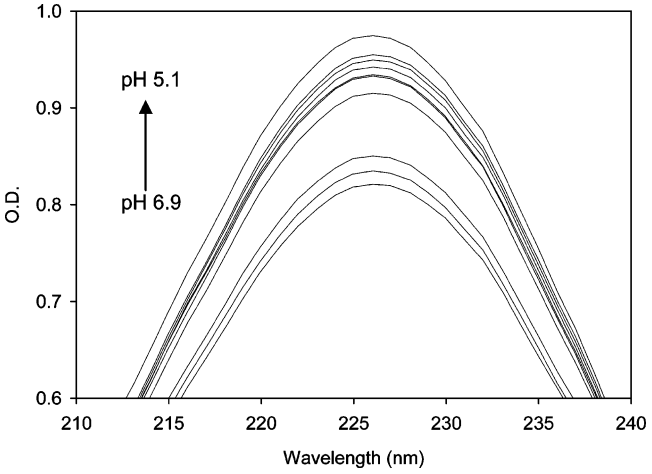

Figure 2. UV−vis absorption of 100 μM DMPO aqueous solution at pH 5.1−6.9 at 25 °C.

SCHEME 2: Mesomeric Forms of PBN

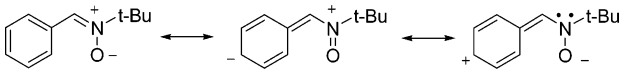

SCHEME 3: Resonance Forms of DMPO−H$^+$

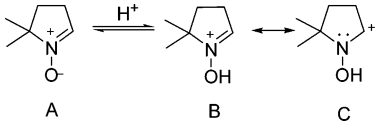

SCHEME 4: Resonance Forms of DMPO

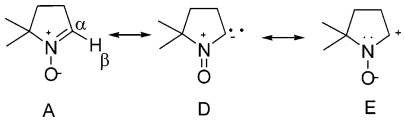

on the oxygen atom can explain the higher basicity of PBN compared to DMPO.

(b) Spectrophotometric Titration. The UV−vis spectral absorbances of DMPO as a function of pH was investigated and are shown in Figure 2. The nature of the absorbance at 227 nm has been assigned[60,61] to the $\pi-\pi^*$ transition of the azomethine system in conjugation with the negatively charged oxygen atom, i.e., HC═N→O. The 227 nm absorbance increases with decreasing pH over the pH range of 4.5−7.5 suggesting a higher molar absorptivity for the protonated nitrone similar to that observed for some carbonyl compounds in acidic pH.[62] The enhanced absorbance at 227 nm can be due to the increased contribution of the resonance forms B and C (Scheme 3) compared to D and E (Scheme 4).

The pK_a for DMPO was determined using

$$\mathrm{p}K_a = \mathrm{pH} + \log \frac{A_I - A}{A - A_M} \qquad (2)$$

where A_I, A_M, and A are the optical absorbances of DMPO−H$^+$, DMPO, and the observed absorbance from pH 5.1 to 6.9, respectively. Based on eq 2, the calculated pK_a is 6.00 ± 0.02 (n = 14) at 100 μM (see Tables S4−S5 of Supporting Information) and 25 °C and is within the experimental error observed for the potentiometrically determined pK_a value of 5.99 ± 0.02, which further validates this pK_a.

B. NMR Studies. ^{1}H NMR spectroscopy was employed to explore the nature of protonation of DMPO. For a weak acid such as DMPO, the NMR chemical shift of the protons close to the protonation site should be pH sensitive because the local electron density around this nucleus should change as the protonation state of the nitronyl moiety changes. Figure 3 shows the ^{1}H NMR chemical shifts of DMPO in the range 1.0−7.25 ppm. No change in the chemical shifts was observed in the range of 1.0−5.0 ppm, which was assigned to the methylene and methyl protons, indicating the absence of electron delocalization on these nuclei. However, the methine proton at 7.12 ppm exhibited a downfield shift as the pH is lowered, which is characterized by deshielding of the methine proton. Scheme 3 shows that the positive charge is distributed between the nitrogen (form B) atom and the α-carbon (form C) to form the *N*-hydroxy imino cation or hydroxylamine bearing an α-carbocation, respectively. The electron density on the methine proton nucleus is relatively lower at acidic pH due to larger contribution of the protonated resonance form C (see Scheme 3), which has no nitronyl group. This ^{1}H NMR study indicates that the site of protonation is the oxygen atom, and therefore, the ion is of *N*-hydroxyl amine (or imine) cation in nature. A similar shift in ^{1}H NMR signal has been observed for the methine protons in aldehydes upon protonation of the carbonyl oxygen.[63]

SCHEME 5: Protonation of DMPO at the α-Carbon

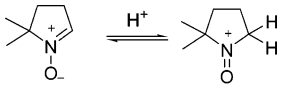

^{13}C NMR spectra were also obtained between the pH range 5−7 and are shown in Figure 4. Results show a similar trend in chemical shift behavior for the nitronyl and quarternary carbon atoms as observed for the nitronyl hydrogen in the ^{1}H NMR study. The downfield change in chemical shift of the nitronyl carbon (143.5 ppm) at lower pH is more evident compared to the quarternary carbon atom (74.8 ppm), further supporting the electron delocalization within the HC═N→O moiety.

The pK_a was also determined on the basis of the observed shifts in the ^{1}H and ^{13}C NMR signals upon protonation. The calculated pK_a is 6.14 ± 0.20 using the proton peak at 7.1 ppm and the carbon peaks at 143.5 and 74.8 ppm yielded pK_a values of 6.12 ± 0.04 and 6.09 ± 0.07, respectively. These results are in good agreement with the pK_a values obtained using potentiometric and spectrophotometric titrations.

C. Computational Studies. ***(a) Protonated DMPO.*** The resonance structures for the unprotonated DMPO exhibit charge delocalization through the resonance forms A, D, and E (Scheme 4). From these resonance forms, two atoms assumed a negative charge, i.e., the oxygen (A) and α-carbon (D), and therefore are possible sites for protonation. Schemes 3 and 5 show the protonation of DMPO to yield the *N*-hydroxy imino cation (B) and oxoammonium (F), respectively, and Figure 5 shows the calculated relative free energies of the protonated forms B and F at the PCM/B3LYP/6-31+G**//B3LYP/6-31G* level. The protonated B-form in *trans* conformation is the most thermodynamically preferred compared to the B-*cis* and F forms by 3.3 and 27.2 kcal/mol, respectively. Compound F gave a C−N bond distance of 1.50 Å, which is longer than the C−N bond distance of 1.28 Å observed in compounds B-*cis* and B-*trans*, or 1.31 Å in DMPO. This prediction further supports the observed increase in UV absorption during protonation indicating larger contribution of the resonance form B.

Natural population analysis at the PCM/B3LYP/6-31+G** level for various nitrones (see Chart 1) gave higher charge density on the α-carbon for the protonated form with charges

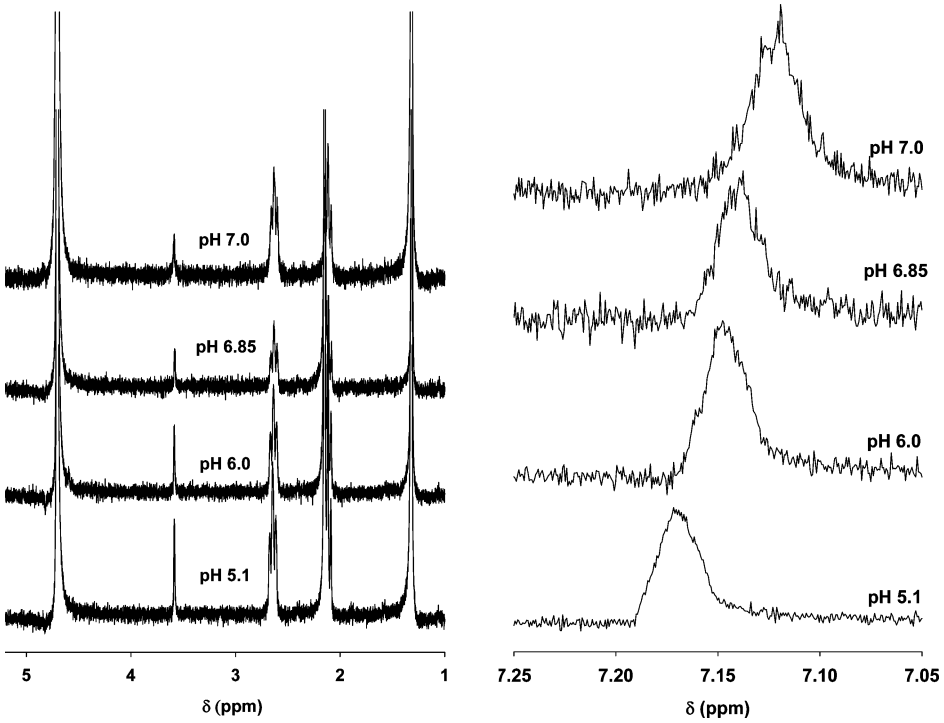

Figure 3. ^{1}H NMR spectrum of methyl and methylene hydrogens (left) and nitronyl hydrogen (right) of DMPO at pH 7.0, 6.85, 6.0, and 5.1 in $D_2SO_4-D_2O$.

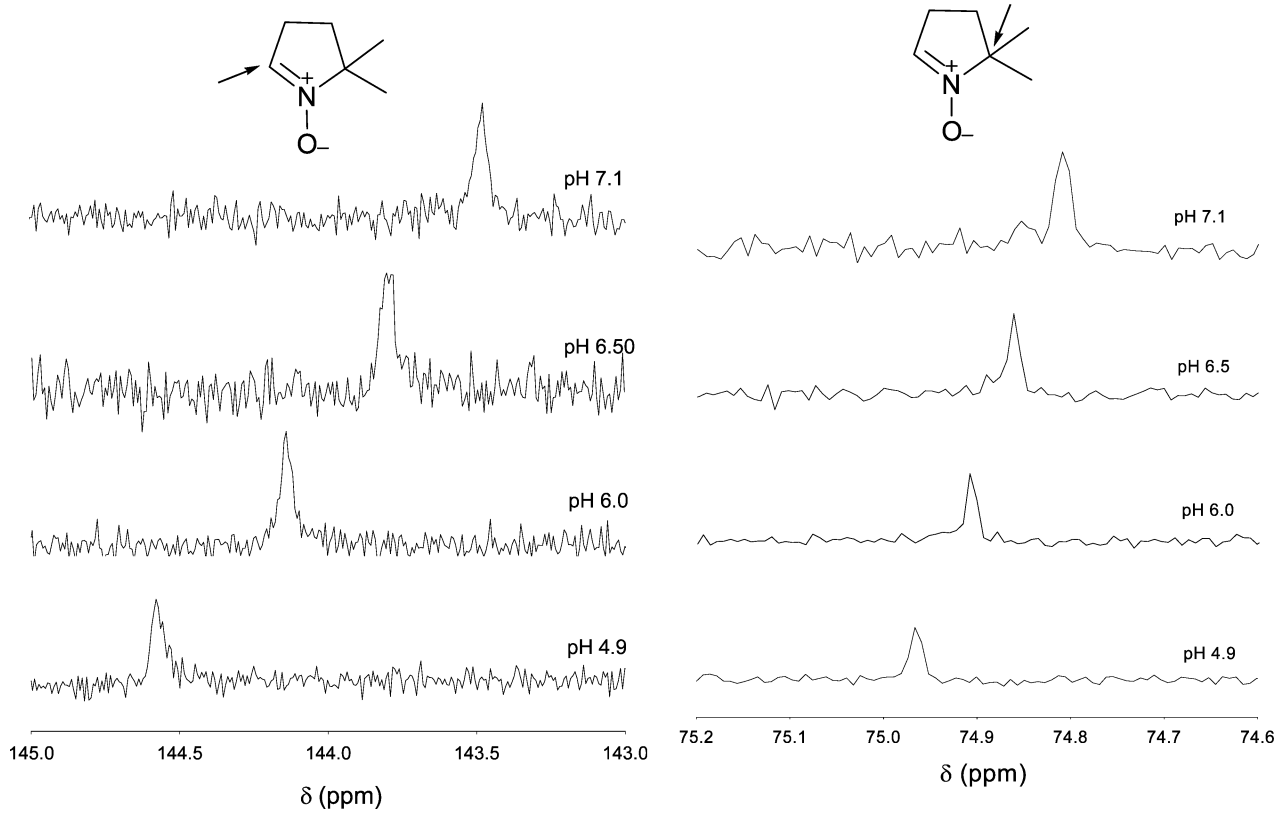

Figure 4. ^{13}C NMR spectrum of the nitronyl carbon (left) and quarternary carbon (right) of DMPO (50 mM) at pH 7.1, 6.5, 6.0, and 4.9 in $D_2SO_4-D_2O$. Peaks are relative to the methyl peak set at 24.6 ppm. Only negligible change in chemical shifts on methylene carbons at 25.4 and 33.6 ppm was observed as a function of pH.

that range from 0.19 to 0.27 e compared to the unprotonated nitrones with charges ranging only from 0.02 to 0.1 e (see Table 1), but there is no significant difference in the charges on the oxygen and nitrogen between the two forms. The increase in the positive charge density on the α-carbon upon protonation can also explain the downfield shift experimentally observed for the methine proton of DMPO at lower pH due to deshielding effect.

(b) Kinetics and Thermodynamics of Superoxide Radical Anion Addition to Protonated DMPO and Other Nitrones. The

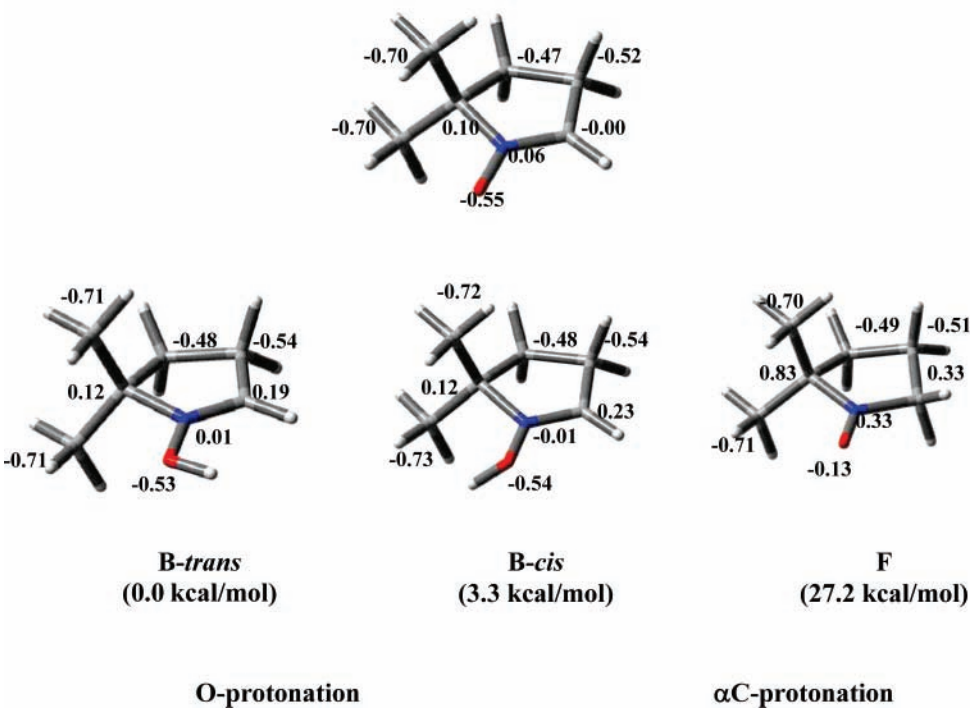

Figure 5. NBO charges of N, C, and O atoms for DMPO (top) and protonated DMPO (bottom) at the PCM/B3LYP/6-31+G**//B3LYP/6-31G* level showing the relative free energies in kcal/mol.

CHART 1: Substituted Cyclic Nitrones

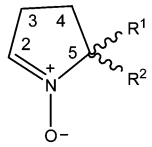

R^1	R^2	Acronym
$-CH_3$	$-CH_3$	DMPO
$-CH_3$	$-CF_3$	TFMPO
$-CH_3$	$-C(O)NH_2$	AMPO
$-CH_3$	$-C(O)NHCH_3$	MAMPO
$-CH_3$	$-C(O)N(CH_3)_2$	DiMAMPO
$-CH_3$	$-CO_2Et$	EMPO
$-CH_3$	$-P(O)(OEt)_2$	DEPMPO
$-CO_2Et$	$-CO_2Et$	DEPO
$-CO_2Et$	$-C(O)NHCHCH_3$	EMAPO
$-C(O)NHCH_3$	$-C(O)NHCH_3$	DiMAPO

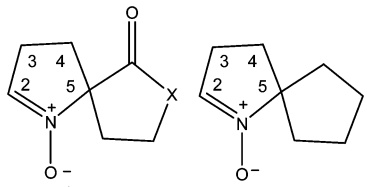

X	Acronym
O	CPCOMPO
N-H	TAMPO

CPPO

10-fold increase in the charge density of the α-carbon for all the nitrones shown in Table 1 can have a significant effect on the energetics of their addition to $O_2^{\bullet-}$. We have previously shown[36] the role of electrostatic effects on the $O_2^{\bullet-}$ addition to nitrones in which the charge density on the α-carbon plays a critical role for the facile addition reaction. Kinetics and thermodynamic data indicate that nitrones with high positive charge on the α-carbon gave more negative free energy and

TABLE 1: NBO Charges of Oxygen, Nitrogen and α-Carbon for Nitrones and Their Respective Protonated Forms at the PCM/B3LYP/6-31+G//B3LYP/6-31G* Level of Theory at 298 K in Aqueous Phase**

	Unprotonated			Protonated		
						
Nitrones	**O**	**N**	**C**	**O**	**N**	**C**
AMPO	-0.53	0.05	0.06	-0.54	0.00	0.22
CPCOMPO	-0.61	0.07	0.05	-0.54	-0.01	0.26
CPPO	-0.63	0.08	0.02	-0.54	0.00	0.23
DEPMPO	-0.62	0.06	0.04	-0.54	-0.03	0.25
DEPO	-0.60	0.08	0.04	-0.53	-0.01	0.24
DiMAMPO	-0.62	0.08	0.03	-0.55	0.00	0.22
DiMAPO	-0.63	0.04	0.10	-0.55	-0.02	0.25
DMPO	-0.63	0.07	0.02	-0.54	0.01	0.19
EMAPO	-0.62	0.05	0.07	-0.54	0.00	0.25
EMPO	-0.61	0.07	0.04	-0.53	-0.01	0.25
MAMPO	-0.63	0.05	0.06	-0.55	0.00	0.22
MSMPO	-0.60	0.04	0.01	-0.54	-0.05	0.27
TAMPO	-0.61	0.07	0.04	-0.54	-0.01	0.25
TFMPO	-0.60	0.06	0.04	-0.52	0.00	0.22

higher second-order rate constants for the $O_2^{\bullet-}$ addition to nitrones.[36] Experimental evidence shows an increase in the rate constant from 2.0 M^{-1} s^{-1} at pH 7.2 to 27.5 M^{-1} s^{-1} at pH 6.2, a 14-fold increase in rate constant.[31] The nitrones, EMPO and DEPO also gave the same behavior with rate constants of 10.9 and 31 M^{-1} s^{-1} at pH 7.2 and 101 and 185 M^{-1} s^{-1} at pH 6.2, respectively.[31] It has been proposed that this increase in rate constants is due to the presence of higher equilibrium concentration of $HO_2^{\bullet}$, which is more oxidizing than its unprotonated form $O_2^{\bullet-}$ (Schemes 6 and 7). The relative reactivity of $O_2^{\bullet-}$ and $HO_2^{\bullet}$ to DMPO was computationally rationalized at the PCM/B3LYP/6-31+G**//B3LYP/6-31G* level.[36,37] The $O_2^{\bullet-}$ addition to DMPO was predicted to be 11.9 kcal/mol[36] endoergic (Scheme 6), and $HO_2^{\bullet}$ addition was exoergic by −4.6 kcal/mol (Scheme 7).[37] The same trend in $O_2^{\bullet-}$ and $HO_2^{\bullet}$ reactivity was predicted at the PCM/mPW1K/6-31+G** levels of theory.[36,37]

SCHEME 6: Free Energies of Reaction (in kcal/mol) for the Superoxide Radical Anion Addition to DMPO in Neutral pH at the PCM/B3LYP/6-31+G//B3LYP/6-31G* at 298 K**

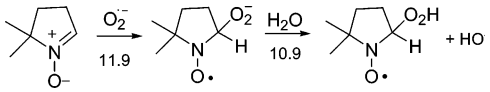

SCHEME 7: Free Energies of Reaction (in kcal/mol) for the Superoxide Radical Anion Addition to DMPO in Acidic Medium at the PCM/B3LYP/6-31+G//B3LYP/6-31G* at 298 K**

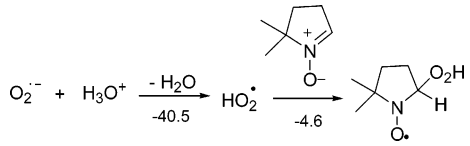

On the basis of the determined pK_a of ~6.0 for DMPO from this work and the established pK_a for $O_2^{\bullet-}$ of 4.8[33] and 4.4,[34] it is possible that the equilibrium concentration of DMPO−H^+ will be higher compared to $HO_2^{\bullet}$ between pH 5.0 and 7.0. Therefore, we further theoretically investigated using DFT approach the effect of protonation of DMPO on its reactivity to $O_2^{\bullet-}$. The two conformational isomers of the $O_2^{\bullet-}$ adduct of DMPO−H^+ are shown in Figure 6. The conformation A (Figure 6, top) in which the −OH moiety is oriented away from the −OO- group is more thermodynamically preferred by −4.7 kcal/mol than conformation B (Figure 6, bottom) in which the −OH and $-OO^-$ group are oriented toward each other.

The electronic property of the DMPO−H^+−O_2^- was examined at the PCM/B3LYP/6-31+G** level and shows that most of the spin density was distributed between the two oxygen atoms of the peroxide moiety, with 32% and 68% spin density distribution at the internal and terminal oxygens, respectively (Table 2). No spin density was observed on the nitrogen and oxygen, indicating that these compounds are not nitroxides in nature, unlike that observed for the $O_2^{\bullet-}$ adduct of DMPO, i.e., DMPO−O_2^-, in which the spin density distribution on the nitrogen and oxygen are higher with 46% on nitrogen, 50% on nitronyl oxygen, 3.0% on internal peroxyl oxygen, and 0% on terminal peroxyl oxygen (see Table 2 for the other $O_2^{\bullet-}$ adducts).[64] The same trend in charge and spin density distribution were observed for various nitrone−H^+−O_2^- adducts with spin densities that range from 31−34% and 66−68% for the internal and terminal oxygens, respectively (Table 2).

An alternative mechanism was, therefore, proposed for $O_2^{\bullet-}$ addition to DMPO at pK_a less than 6.0, as shown in Table 3. Data show that the protonation of DMPO (Table 3, reaction A) is exoergic with $\Delta G_{rxn,aq,298K} = -26.4$ kcal/mol and subsequent addition of $O_2^{\bullet-}$ to DMPO−H^+ to form DMPO−H^+−O_2^- is exoergic by 4.6 kcal/mol (Table 3, reaction B). Proton transfer from the nitronyl oxygen to the peroxyl oxygen to form DMPO−O_2H is also exoergic with $\Delta G_{rxn,aq,298K}$ of −13.7 kcal/mol. The overall free energy for the formation of DMPO−O_2H via DMPO−H^+ is $\Delta G_{total} = -44.7$ kcal/mol, which is more favorable than the formation of DMPO−O_2H via direct addition of $O_2^{\bullet-}$ to DMPO (Scheme 6) with total endoergic free energy of 22.8 kcal/mol but is slightly less favorable than the direct addition of $HO_2^{\bullet}$ to DMPO (Scheme 7) with $\Delta G_{total} = -45.1$ kcal. These thermodynamic data suggest that the addition reaction of $O_2^{\bullet-}$ to DMPO−H^+ can compete with the addition of $HO_2^{\bullet}$ to DMPO in mildly acidic pH.

For all the nitrones considered in Table 3, the average ΔG_{total} for the formation of nitrone−O_2H via the direct addition of $HO_2^{\bullet}$ to nitrone is only 0.45 ± 0.06 kcal/mol more exoergic than the nitrone−O_2H formation from the addition of $O_2^{\bullet-}$ to nitrone−H^+. Although there is no significant difference in the charge densities on the nitronyl carbon for various protonated nitrones (Table 2), the free energies of $O_2^{\bullet-}$ addition to nitrone−H^+ vary significantly with $\Delta G_{rxn,aq,298K}$ that range from −4.4 to −17.6 kcal/mol (see Table 3, reaction B) with $O_2^{\bullet-}$ addition to DMPO and DiMAMPO to be the most endoergic and CPCOMPO and MSMPO to be most exoergic. In comparison to $HO_2^{\bullet}$ addition to unprotonated nitrones, the $\Delta G_{rxn,aq,298K}$ only range from −0.9 to −7.3.[37] None of the nitrone−H^+−O_2^- adducts exhibits intramolecular H-bonding interaction because the preferred conformation is similar to that observed for the DMPO−H^+−O_2^- (Figure 6, top) in which the $-OO^-$ moiety is oriented in the opposite direction from the −NOH group. Rationale for the varying favorability of $O_2^{\bullet-}$ addition to various nitrone−H^+'s is unclear at the moment but is neither electrostatic nor driven by the formation of intramolecular H-bonding interaction as demonstrated for the addition of $O_2^{\bullet-}$ and/or $HO_2^{\bullet}$ to unprotonated nitrones.[36,37]

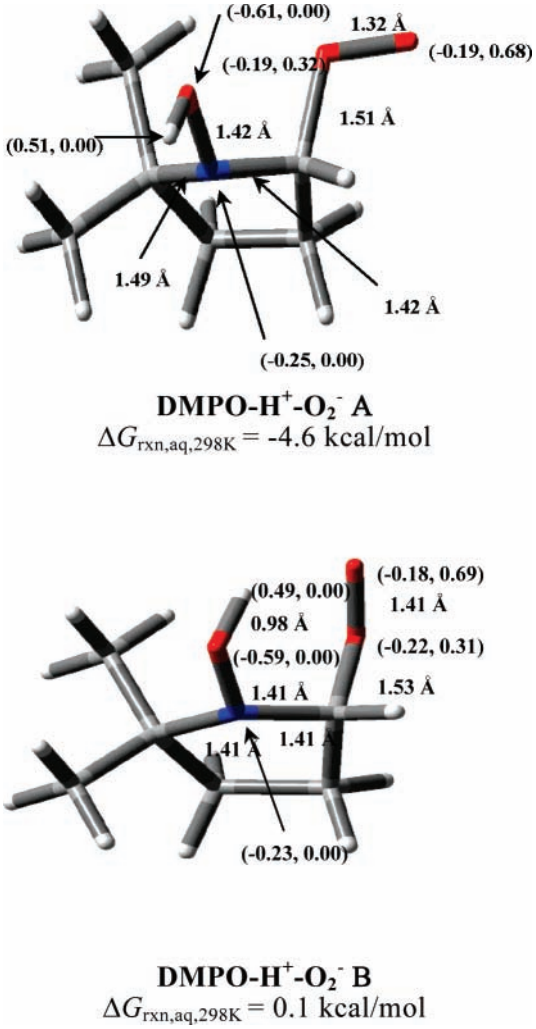

Figure 6. Optimized conformational isomers of the superoxide radical anion adduct of DMPO−H^+ showing reaction free energies, (charge density, spin density) and pertinent bond lengths at the PCM/B3LYP/6-31+G**//B3LYP/6-31G* level.

(c) Predicted Ionization Constants. Table 4 shows the approximated ionization constants for the conjugate acids of various nitrones using the same computational method employed for the determination of the pK_a of hydroperoxyl,[56] hydroxyl,[65] the carbon dioxide anion,[65] and the carbonate anion[66] radical

TABLE 2: NBO Spin and Charge (in Parentheses) Densities of Nitronyl Oxygen (O_N), Nitrogen (N), Internal Peroxyl Oxygen (O_I), and Terminal Oxygen (O_T) for Various Superoxide Adducts of Nitrones and of Their Respective Protonated Forms at the PCM/B3LYP/6-31+G//B3LYP/6-31G* Level of Theory at 298 K in Aqueous Phase**

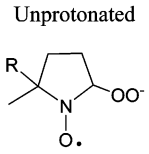

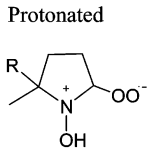

Nitrones	O_N	N	O_I	O_T	O_N	N	O_I	O_T
AMPO	0.48 (-0.47)	0.46 (0.00)	0.03 (-0.36)	0.00 (-0.57)	0.00 (-0.65)	0.00 (-0.26)	0.33 (-0.17)	0.66 (-0.22)
CPCOMPO	0.50 (-0.46)	0.43 (-0.01)	0.03 (-0.42)	0.02 (-0.76)	0.00 (-0.64)	0.00 (-0.24)	0.34 (-0.17)	0.66 (-0.22)
CPPO	0.46 (-0.50)	0.46 (0.01)	0.03 (-0.43)	0.03 (-0.77)	0.00 (-0.65)	0.00 (-0.24)	0.35 (-0.18)	0.65 (-0.23)
DEPMPO	0.49 (-0.46)	0.42 (-0.04)	0.04 (-0.41)	0.04 (-0.76)	0.00 (-0.61)	0.00 (-0.25)	0.33 (-0.20)	0.67 (-0.21)
DEPO	0.49 (-0.46)	0.44 (0.00)	0.04 (-0.35)	0.00 (-0.43)	0.00 (-0.63)	0.01 (-0.24)	0.31 (-0.18)	0.68 (-0.20)
DiMAMPO	0.48 (-0.47)	0.44 (-0.02)	0.05 (-0.40)	0.02 (-0.75)	0.00 (-0.64)	0.00 (-0.25)	0.34 (-0.17)	0.65 (-0.23)
DiMAPO	0.50 (-0.45)	0.45 (0.01)	0.03 (-0.36)	0.00 (-0.56)	0.00 (-0.62)	0.00 (-0.25)	0.33 (-0.17)	0.66 (-0.22)
DMPO	0.46 (-0.51)	0.50 (0.00)	0.03 (-0.42)	0.00 (-0.74)	0.00 (-0.65)	0.00 (-0.25)	0.35 (-0.18)	0.65 (-0.23)
EMAPO	0.52 (-0.43)	0.42 (0.00)	0.04 (-0.36)	0.00 (-0.56)	0.00 (-0.62)	0.00 (-0.24)	0.34 (-0.17)	0.66 (-0.22)
EMPO	0.49 (-0.47)	0.45 (0.00)	0.03 (-0.43)	0.03 (-0.76)	0.00 (-0.64)	0.00 (-0.25)	0.34 (-0.17)	0.66 (-0.22)
MAMPO	0.51 (-0.43)	0.45 (-0.02)	0.03 (-0.37)	0.00 (-0.64)	0.00 (-0.65)	0.00 (-0.25)	0.34 (-0.17)	0.66 (-0.22)
MSMPO	n/a[a]	n/a	n/a	n/a	0.00 (-0.62)	0.00 (-0.27)	0.33 (-0.16)	0.66 (-0.21)
TAMPO	0.49 (-0.47)	0.45 (0.00)	0.03 (-0.43)	0.02 (-0.77)	0.00 (-0.64)	0.01 (-0.24)	0.33 (-0.17)	0.67 (-0.21)
TFMPO	0.51 (-0.45)	0.42 (-0.02)	0.04 (-0.43)	0.03 (-0.75)	0.00 (-0.64)	0.00 (-0.25)	0.34 (-0.17)	0.66 (-0.22)

[a] Resulted in the nucleophilc substitution of sulfonyl group.

TABLE 3: Reaction Free Energies of Superoxide Radical Anion ($O_2^{\bullet-}$) Addition to Protonated Nitrones[a] To Form the Hydroperoxyl Adducts at the PCM/B3LYP/6-31+G// B3LYP/6-31G* Level at 298 K in Aqueous Phase**

Reaction Free Energies ($\Delta G_{rxn,298K,aq}$ in kcal/mol)

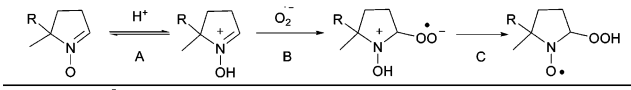

Nitrone[a]	A	B	C
AMPO	-23.8	-7.4	-10.4
CPCOMPO	-16.8	-17.4	-10.5
CPPO	-24.2	-6.5	-14.2
DEPMPO	-18.3	-11.8	-14.8
DEPO	-21.4	-12.1	-12.8
DiMAMPO	-27.7	-4.4	-12.7
DiMAPO	-20.0	-12.3	-10.5
DMPO	-26.4	-4.6	-13.7
EMAPO-*cis*	-20.6	-10.4	-10.0
EMAPO-*trans*	-20.6	-6.7	-17.3
EMPO	-19.8	-13.2	-13.2
MAMPO	-24.5	-6.8	-9.5
MSMPO	-18.2	-17.6	-11.6
TAMPO	-19.5	-12.0	-13.5
TFMPO	-21.6	-12.1	-12.1

[a] See Chart 1 for the corresponding structures.

TABLE 4: Calculated pK_a Values and Their Respective Deprotonation Energies and Solvation Energies

nitrone[a]	$\Delta G_{(gas)}$,[b] kcal/mol	$\Delta\Delta G_{(solv)}$,[c] kcal/mol	calcd[d] pK_a
AMPO	218.1	52.3	8.6
CPCOMPO	211.8	53.7	6.0
CPPO	218.4	48.5	6.7
DEPMPO	223.4	40.7	5.2
DEPO	226.6	39.1	6.0
DiMAMPO	232.7	41.3	10.5
DiMAPO	220.9	47.6	7.6
DMPO−B-cis	217.3	48.7	6.2
DMPO−B-trans	215.6	47.7	4.8
EMAPO	221.7	42.0	5.0
EMPO	216.4	45.4	4.0
MAMPO	212.3	48.3	3.3
MSMPO	220.9	48.8	8.2
TAMPO	218.3	48.8	6.8
TFMPO	207.5	53.1	3.3

[a] Based on the most preferred nitrone−H^+ conformations. [b] Bottom-of-the-well energy plus scaled ZPE at the B3LYP/6-311+G* level. [c] Bottom-of-the-well energy using B3LYP/6-311+G* level and PCM/B3LYP/6-311+G* level. [d] From the linear regression pK_a = 0.538($\Delta G_{aq,AH}$) − 136.9 (r^2 = 0.95 and σ = 0.8 pK_a units).[56]

adducts of DMPO. The predicted pK_a for the B-*trans* and B-*cis* isomers of DMPO−H^+ are 4.8 and 6.2, respectively, and are in reasonable agreement with that obtained experimentally of ~6.0. However, the acidity of all other nitrones gave a wide range of pK_a values from 3.3 to 10.5 with MAMPO and TFMPO being the most acidic and DiMAMPO the most basic. Although most of the substituents are electron-withdrawing, there is a significant variation in the acidity of these nitrones, due perhaps to the high sensitivity of the acid form to the field effect of the substituents. Factors such as hydrogen bonding and medium effect should be taken into account, however, in determining a more accurate pK_a value. A more thorough study on the relative

acidity of the various nitrones presented here is now being investigated in our laboratory.

IV. Conclusion

The pK_a for DMPO was determined to be 6.0 using spectrophotometric, potentiometric, NMR, and computational methods. ^{1}H and ^{13}C NMR studies show a deshielding effect on the methine hydrogen and nitronyl carbon, respectively, upon acidification, suggesting increased positivity of the nitronyl carbon. DFT studies revealed that the preference for H^+ addition to DMPO is at the oxygen atom to form the *N*-hydroxy imino cation. The NBO charge on the nitronyl carbon of DMPO$-H^+$ increases almost 10-fold compared to DMPO, and the $O_2^{\bullet-}$ addition to DMPO$-H^+$ is exoergic by 4.6 kcal/mol. Thermodynamic data suggest that the addition reaction of $O_2^{\bullet-}$ to DMPO$-H^+$ can compete with the addition of $HO_2^{\bullet}$ to DMPO in mildly acidic pH. This alternative mechanism for $O_2^{\bullet-}$ addition to nitrones can explain their high reactivity at pH below the pK_a of $O_2^{\bullet-}$ and is therefore important in rationalizing the potential antioxidant property of nitrones as $O_2^{\bullet-}$ scavengers in mildly acidic pH. This finding could also provide additional mechanism for the DMPO$-O_2H$ formation for more improved rate laws and more accurate rate constant determination of $O_2^{\bullet-}$ trapping by nitrones.

The issue of nitrone cellular permeability, however, will determine whether this radical scavenging property in mildly acidic pH is relevant intracellularly. Although DMPO has been shown to compartmentalize inside the cytosol using isolated rat atria[67] or lyposomes,[67] the high buffering power of the cytosol may not favor this mechanism. Nevertheless, the location of $O_2^{\bullet-}$ production, i.e., whether extracellular versus intracellular, may have varying pathophysiological effects because extracellularly generated $O_2^{\bullet-}$ may affect adjacent cells and inactivate NO in the vasculature, and on the other hand, intracellularly generated $O_2^{\bullet-}$ may cause dysfunction of the cells that produce it. In both conditions, the favorable $O_2^{\bullet-}$ scavenging by nitrones in mildly acidic condition may have pharmacological significance and warrants further investigation.

Acknowledgment. This publication was made possible by grant number HL 81248 from the NIH National Heart, Lung, and Blood Institute. This work was supported in part by an allocation of computing time from the Ohio Supercomputer Center.

Supporting Information Available: Potentiometric and spectrophotometric titration and^{1}H and ^{13}C NMR data as well as energies, enthalpies, and free energies for all spin traps and their corresponding spin adducts are available as Supporting Information. This information is available free of charge at http://pubs.acs.org.

References and Notes

(1) Halliwell, B.; Gutteridge, J. M. C. *Free Radicals in Biology and Medicine*; Oxford University Press: New York, 1999.

(2) Zweier, J. L.; Villamena, F. A. Chemistry of free radicals in biological systems. In *Oxidative Stress and Cardiac Failure*; Kukin, M. L., Fuster, V., Eds.; Futura Publishing: Armonk, NY, 2003; pp 67.

(3) Zweier, J. L.; Broderick, R.; Kuppusamy, P.; Thompson-Gorman, S.; Lutty, G. A. *J. Biol. Chem.* **1994**, *269*, 24156.

(4) Zweier, J. L.; Flaherty, J. T.; Weisfeldt, M. L. *Proc. Natl. Acad. Sci. U.S.A.* **1987**, *84*, 1404.

(5) Zweier, J. L.; Kuppusamy, P.; Williams, R.; Rayburn, B. K.; Smith, D.; Weisfeldt, M. L.; Flaherty, J. T. *J. Biol. Chem.* **1989**, *264*, 18890.

(6) Ambrosio, G.; Zweier, J. L.; Flaherty, J. T. *J. Mol. Cell Cardiol.* **1991**, *23*, 1359.

(7) Crampin, E. J.; Smith, N. P.; Langham, A. E.; Clayton, R. H.; Orchard, C. H. *Math. Phys. Eng. Sci.* **2006**, *364*, 1171.

(8) Fukumura, D.; Jain, R. K. *J. Cell. Biochem.* **2007**, *101*, 937.

(9) Kim, B.; Forbes, N. S. *Biotechnol. Bioeng.* **2007**, *96*, 1167.

(10) Pastorekova, S.; Kopacek, J.; Pastorek, J. *Curr. Top. Med. Chem.* **2007**, *7*, 865.

(11) Becker, D. A.; Ley, J. J.; Echegoyen, L.; Alvarado, R. *J. Am. Chem. Soc.* **2002**, *124*, 4678.

(12) Floyd, R. A. *Aging Cell* **2006**, *5*, 51.

(13) Ginsberg, M. D.; Becker, D. A.; Busto, R.; Belayev, A.; Zhang, Y.; Khoutorova, L.; Ley, J. J.; Zhao, W.; Belayev, L. *Ann. Neurol.* **2003**, *54*, 330.

(14) Nakae, D.; Kishida, H.; Enami, T.; Konishi, Y.; Hensley, K. L.; Floyd, R. A.; Kotake, Y. *Cancer Sci.* **2003**, *94*, 26.

(15) Nakae, D.; Uematsu, F.; Kishida, H.; Kusuoka, O.; Katsuda, S.-i.; Yoshida, M.; Takahashi, M.; Maekawa, A.; Denda, A.; Konishi, Y.; Kotake, Y.; Floyd, R. A. *Cancer Lett.* **2004**, *206*, 1.

(16) Floyd, R. A.; Hensley, K. *Ann. N. Y. Acad. Sci.* **2000**, *899*, 222.

(17) Packer, L.; Cadenas, E. *Handbook of Synthetic Antioxidants*; Marcel Dekker, Inc.: New York, 1997.

(18) Paracchini, L.; Jotti, A.; Bottiroli, G.; Prosperi, E.; Supino, R.; Piccinini, F. *Anticancer Res.* **1993**, *3*, 1607.

(19) von Frijtag, J. K.; Kunzel, D.; van der Zee, J.; Ijzerman, A. P. *Drug Dev. Res.* **1996**, *37*, 48.

(20) Zucchi, R.; Ghelardoni, S.; Evangelista, S. *Curr. Med. Chem.* **2007**, *14*, 1619.

(21) Bradamante, S.; Jotti, A.; Paracchini, L.; Morti, E. *Eur. J. Pharmacol.* **1993**, *234*, 113.

(22) Maurelli, E.; Culcasi, M.; Delmas-Beauvieux, M.-C.; Miollan, M.; Gallis, J.-L.; Tron, T.; Pietri, S. *Free Radic. Biol. Med.* **1999**, *27*, 34.

(23) Pietri, S.; Liebgott, T.; Frijaville, C.; Tordo, P.; Culcasi, M. *Eur. J. Biochem.* **1998**, *254*, 256.

(24) Tosaki, A.; Blasig, I. E.; Pali, T.; Ebert, B. *Free Radic. Biol. Med.* **1990**, *8*, 363.

(25) Tosaki, A.; Braquet, P. *Am. Heart J.* **1990**, *120*, 819.

(26) Tosaki, A.; Haseloff, R. F.; Hellegouarch, A.; Schoenheit, K.; Martin, V. V.; Das, D. K.; Blasig, I. E. *Basic Res. Cardiol.* **1992**, *87*, 536.

(27) Anderson, D. E.; Yuan, X. J.; Tseng, C. M.; Rubin, L. J.; Rosen, G. M.; Tod, M. L. *Biochem. Biophys. Res. Commun.* **1993**, *193*, 878.

(28) Konorev, E. A.; Baker, J. E.; Joseph, J.; Kalyanaraman, B. *Free Radic. Biol. Med.* **1993**, *14*, 127.

(29) Bolli, R. *J. Mol. Cell. Cardiol.* **2001**, *33*, 1897.

(30) Locigno, E. J.; Zweier, J. L.; Villamena, F. A. *Org. Biomol. Chem.* **2005**, *3*, 3220.

(31) Allouch, A.; Lauricella, R. P.; Tuccio, B. N. *Mol. Phys.* **2007**, *105*, 2017.

(32) Finkelstein, E.; Rosen, G. M.; Rauckman, E. J. *J. Am. Chem. Soc.* **1980**, *102*, 4995.

(33) Behar, D.; Czapski, G.; Rabani, J.; Dorfman, L. M.; Schwarz, H. A. *J. Phys. Chem.* **1970**, *74*, 3209.

(34) Czapski, G.; Bielski, B. H. J. *J. Phys. Chem.* **1963**, *67*, 2180.

(35) Buettner, G. R. *Arch. Biochem. Biophys.* **1993**, *300*, 535.

(36) Villamena, F. A.; Xia, S.; Merle, J. K.; Lauricella, R.; Tuccio, B.; Hadad, C. M.; Zweier, J. L. *J. Am. Chem. Soc.* **2007**, *129*, 8177.

(37) Villamena, F. A.; Merle, J. K.; Hadad, C. M.; Zweier, J. L. *J. Phys. Chem. A* **2007**, *111*, 9995.

(38) Xiong, Z.-G.; Zhu, X.-M.; Chu, X.-P.; Minami, M.; Hey, J.; Wei, W.-L.; MacDonald, J. F.; Wemmie, J. A.; Price, M. P.; Welsh, M. J.; Simon, R. P. *Cell* **2004**, *118*, 687.

(39) Simonis, G.; Marquetant, R.; Rothele, J.; Strasser, R. H. *Cardiovasc. Res.* **1998**, *38*, 646.

(40) Pacini, D. J.; Kane, K. A. *J. Cardiovasc. Pharmacol.* **1991**, *18*, 261.

(41) Altschuld, R. A.; Hostetler, J. R.; Brierley, G. P. *Circ. Res.* **1981**, *49*, 307.

(42) Labanowski, J. W.; Andzelm, J. *Density Functional Methods in Chemistry*; Springer: New York, 1991.

(43) Parr, R. G.; Yang, W. *Density Functional Theory in Atoms and Molecules*; Oxford University Press: New York, 1989.

(44) Becke, A. D. *Phys. Rev.* **1988**, *38*, 3098.

(45) Lee, C.; Yang, W.; Parr, R. G. *Phys. Rev. B* **1988**, *37*, 785.

(46) Becke, A. D. *J. Chem. Phys.* **1993**, *98*, 1372.

(47) Hehre, W. J.; Radom, L.; Schleyer, P. V.; Pople, J. A. *Ab Initio Molecular Orbital Theory*; John Wiley & Sons: New York, 1986.

(48) Barone, V.; Cossi, M.; Tomasi, J. *J. Chem. Phys.* **1997**, *107*, 3210.

(49) Barone, V.; Cossi, M.; Tomasi, J. *J. Comput. Chem.* **1998**, *19*, 404.

(50) Cossi, M.; Barone, V.; Cammi, R.; Tomasi, J. *Chem. Phys. Lett.* **1996**, *255*, 327.

(51) Tomasi, J.; Mennucci, B.; Cammi, R. *Chem. Rev.* **2005**, *105*, 2999.

(52) Tomasi, J.; Persico, M. *Chem. Rev.* **1994**, *94*, 2027.

(53) Frisch, M. J.; et al. *Gaussian 03*, revision B.04 ed.; Gaussian, Inc.: Pittsburgh, PA, 2003.

(54) Reed, A. E.; Curtiss, L. A.; Weinhold, F. A. *Chem. Rev.* **1988**, *88*, 899.
(55) Scott, A. P.; Radom, L. *J. Phys. Chem.* **1996**, *100*, 16502.
(56) Villamena, F. A.; Merle, J. K.; Hadad, C. M.; Zweier, J. L. *J. Phys. Chem. A* **2005**, *109*, 6083.
(57) Albert, A.; Serjeant, E. P. *The Determination of Ionization Constants: A Laboratory Manual*, 3rd ed.; Chapman and Hall: New York, 1984.
(58) Lide, D. R. *CRC Handbook of Chemistry and Physics*; CRC Press: Boca Raton, FL, 2002.
(59) Torssell, K. B. G. *Nitrile Oxides, Nitrones, and Nitronates in Organic Synthesis: Novel Strategies in Synthesis*; VCH: New York, 1988.
(60) Hamer, J.; Macaluso, A. *Chem. Rev.* **1964**, *64*, 473.
(61) Kaminsky, L. S.; Lamchen, M. *J. Chem. Soc. B: Phys. Org.* **1968**, 1085.
(62) Yates, K.; Stewart, R. *Can. J. Chem.* **1959**, *37*, 664.
(63) Olah, G. A.; Halpern, Y.; Mo, Y. K.; Liang, G. *J. Am. Chem. Soc.* **1972**, *94*, 3554.
(64) Villamena, F. A.; Hadad, C. M.; Zweier, J. L. *J. Phys. Chem. A* **2005**, *109*, 1662.
(65) Villamena, F. A.; Locigno, E. J.; Rockenbauer, A.; Hadad, C. M.; Zweier, J. L. *J. Phys. Chem. A* **2006**, *110*, 13253.
(66) Villamena, F. A.; Locigno, E. J.; Rockenbauer, A.; Hadad, C. M.; Zweier, J. L. *J. Phys. Chem. A* **2007**, 384.
(67) Anzai, K.; Aikawa, T.; Furukawa, Y.; Matsushima, Y.; Urano, S.; Ozawa, T. *Arch. Biochem. Biophys.* **2003**, *415*, 251.